Short-Range Interactions within Molecular Complexes Formed in Supersonic Beams: Structural Effects and Chiral Discrimination

Andrea Latini,[b] Mauro Satta,[b] Anna Giardini Guidoni,[b] Susanna Piccirillo,[c] and Maurizio Speranza*[a]

Abstract: One- and two-color, mass-selected R2PI spectra of the $S_1 \leftarrow S_0$ transitions in the bare chiral chromophore *R*-(+)-1-phenyl-1-propanol (**R**) and its complexes with a variety of alcoholic solvent molecules (**solv**), namely methanol, ethanol, 1-propanol, 2-propanol, 1-butanol, *S*-(+)-2-butanol, *R*-(−)-2-butanol, 1-pentanol, *S*-(+)-2-pentanol, *R*-(−)-2-pentanol, and 3-pentanol, were recorded after a supersonic molecular beam expansion. Spectral analysis, coupled with theoretical calculations, indicate that several hydrogen-bonded [**R**·**solv**] conformers are present in the beam. The R2PI excitation spectra of [**R**·**solv**] are characterized by significant shifts of their band origin relative to that of bare **R**. The extent and direction of these spectral shifts depend on the structure and configuration of **solv** and are attributed to different short-range interactions in the ground and excited [**R**·**solv**] complexes. Measurement of the binding energies of [**R**·**solv**] in their neutral and ionic states points to a subtle balance between attractive (electrostatic and dispersive) and repulsive (steric) forces, which control the spectral features of the complexes and allow enantiomeric discrimination of chiral **solv** molecules.

Keywords: chiral recognition · cluster energetics · enantiomeric resolution · mass spectrometry

Introduction

Chiral recognition is a fundamental phenomenon in chemistry and biology and is based on the different affinities of a chiral selector for each member of an enantiomeric pair. Aggregation with the selector leads to diastereomeric molecular complexes (MC), which are generally endowed with different physical and chemical properties as a result of the operation of various short-range intracomplex forces. The characterization of these forces in solution under normal conditions and the investigation of their dependence upon structural factors are difficult, because of the transient character of the MC and the unavoidable interference from the solvent. A way to overcome these difficulties is to generate diastereomeric MC in the isolated state and to characterize the intracomplex forces by spectroscopic methods. The MC between chiral 2-naphthyl-1-ethanol and some aliphatic alcohols have been investigated by Lahmani and co-workers, by using laser-induced fluorescence (LIF) and hole-burning (HB) spectroscopy.[1–3] We could discriminate between the diastereomeric MC between *R*-(+)-1-phenyl-1-propanol (**R**) and *R*-(−)- or *S*-(+)-2-X-butane (X = OH, NH_2)[4–6] on the basis of their spectra, and we measured their interaction energy[7] with the use of resonance-enhanced two-photon ionization (R2PI) spectroscopy,[8–11] coupled with time-of-flight (TOF) detection.[12–14]

Both Lahmani's and our procedure involve formation of weakly bound MC, otherwise unobservable at room temperature, by supersonic expansion of a carrier gas seeded with the two chiral alcohols through a pulsed nozzle. There are many advantages to this method of forming isolated MC. Firstly, only the lowest rotational and vibrational levels in the electronic ground state of MC are populated and, therefore, the spectra often display only a few well-resolved peaks. Furthermore, the photochemical and photophysical properties can be studied without any interference from the environment. Finally, the low internal temperature of the supersonically expanded MC, ranging around a few Kelvins,[13, 14] favors population of the enthalpically most stable MC structural isomer and sometimes stabilization of other

[a] Prof. M. Speranza
Facoltà di Farmacia, Dipartimento di Studi di Chimica e Tecnologia delle Sostanze Biologicamente Attive
Università degli Studi di Roma "La Sapienza"
P.le A. Moro 5, 00185 Roma (Italy)
Fax: (+39) 06-49913602
E-mail: speranza@axrma.uniroma1.it

[b] Dr. A. Latini, Dr. M. Satta, Prof. A. Giardini Guidoni
Dipartimento di Chimica
Università degli Studi di Roma "La Sapienza"
P.le A. Moro 5, 00185 Roma (Italy)

[c] Dr. S. Piccirillo
Dipartimento di Scienze e Tecnologie Chimiche
Università degli Studi di Roma "Tor Vergata"
Roma (Italy)

  0947-6539/00/0606-1042 $ 17.50+.50/0

structural variants, if high-energy barriers need to be overcome for them to interconvert.

The MC considered in the present work were studied by R2PI experiments (Figure 1). One-color R2PI (1cR2PI) experiments involve excitation of the MC to its discrete S_1 state, by absorption of one photon of frequency ν_1, and to the ionization continuum, by absorption of another photon with the same frequency ν_1. The 1cR2PI excitation spectra were obtained by recording the entire TOF mass spectrum as a function of ν_1. The wavelength dependence of a given mass-resolved ion represents the absorption spectrum of the species and contains important information about its electronic excited state S_1. Two-color R2PI (2cR2PI) excitation spectra, on the other hand, involve excitation of MC to its discrete S_1 state, by absorption of one photon of frequency ν_1, and to the ionization continuum, by absorption of a second photon of different frequency ν_2 (Figure 1). The experimental procedure is the following: once the 1cR2PI-TOF mass spectrum of the selected species at the resonant frequency ν_1 has been obtained, the intensity of the laser emitting at ν_1 is lowered to such an extent as to reduce the TOF ion pattern to less than 10%. Then, by superimposing a second laser of frequency ν_2, one assists a pronounced increase in the TOF signal of a characteristic ion only when the 2cR2PI process takes place. The excitation spectra of a given complex is obtained by fixing ν_2 at a value slightly above the ionization threshold and by scanning ν_1. In this way, no significant excess energy is imparted to the complex and decomposition of conceivable higher order clusters is avoided. The ionization threshold of a given species corresponds to the signal onset, which is obtained by scanning ν_2 while keeping ν_1 at the fixed value corresponding to the $S_1 \leftarrow S_0$ transition.

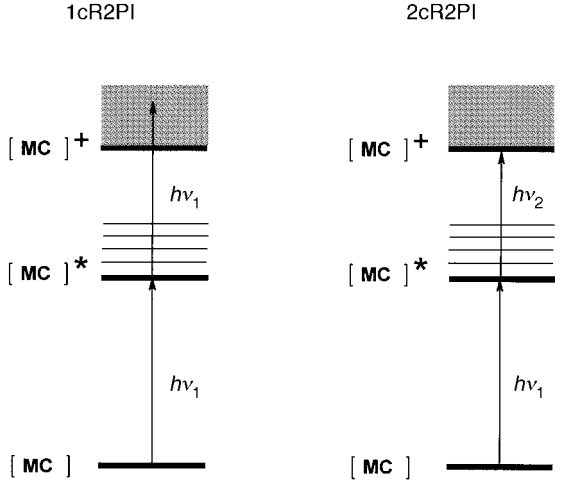

Figure 1. Schematic diagram for 1cR2PI and 2cR2PI experiments.

Comparison of the R2PI spectra of the mass-resolved MC with that of the bare aromatic chromophore provides information about the nature of the interactions operating in MC. The relative contributions of attractive and repulsive short-range forces in isolated MC are determined by careful analysis of the relevant R2PI spectral information in the light of the binding energies of the MC in their ground and excited states.

In this paper we report on a comprehensive R2PI spectroscopic study of the short-range forces operating in the MC between the chromophore **R** and a set of primary and secondary alcohols (**solv**). Comparison of the relevant spectroscopic results with pertinent LIF, HB, and theoretical data[1–3] can hopefully shed some light on the dependence of these forces on the structural and stereochemical features of both the chromophore and the solvating aliphatic alcohol.

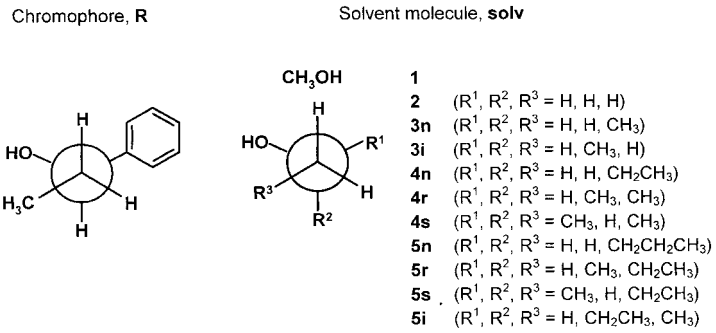

Abstract in Italian: *Sono stati investigati gli spettri di ionizzazione bifotonica risonante (R2PI) a uno e due colori delle transizioni $S_1 \leftarrow S_0$ del cromoforo R-(+)-1-fenil-1-propanolo (**R**) allo stato isolato e dei suoi complessi con alcune molecole alcooliche (**solv**), quali metanolo, etanolo, 1-propanolo, 2-propanolo, 1-butanolo, S-(+)-2-butanolo, R-(−)-2-butanolo, 1-pentanolo, S-(+)-2-pentanolo, R-(−)-2-pentanolo, and 3-pentanolo, in un fascio molecolare espanso supersonicamente. L'analisi spettroscopica, supportata da calcoli teorici, indica la presenza nel fascio supersonico di alcuni conformeri degli addotti molecolari [**R** · **solv**]. Gli spettri di eccitazione di [**R** · **solv**] sono caratterizzati da significative deviazioni delle loro bande fondamentali rispetto a quelle dei rotameri di **R**. L'entità e la direzione di tali deviazioni risultano dipendenti dalla struttura e dalla configurazione di **solv** e sono attribuite alle diverse interazioni intime presenti nei complessi [**R** · **solv**] allo stato fondamentale ed eccitato. La misura delle energie di interazione in [**R** · **solv**] allo stato neutro e ionizzato rivela una sottile interdipendenza tra le forze attrattive (elettrostatiche e di polarizzazione) e repulsive (steriche) che sono responsabili delle caratteristiche spettroscopiche dei complessi e che permettono la discriminazione fra le forme enantiomeriche di **solv** chirali.*

Experimental Section

Mass-selected R2PI spectroscopy: The experimental setup for the generation of the adducts between **R** and **solv** and for their R2PI/TOF analysis was described previously.[13–15] Supersonic-beam production of the adducts was obtained by adiabatic expansion of a carrier gas (Ar) seeded with *R*-(+)-1-phenyl-1-propanol (**R**) and the corresponding alcohols **solv** (Aldrich Chemical Co.), through a pulsed (aperture time: 200 μs; repetition rate: 10 Hz) 400 μm i.d. nozzle heated at 80 °C. The **solv** concentration was always maintained low enough to minimize the contribution of heavier

clusters to the spectra. The molecular beam was allowed to pass through a 1 mm skimmer into a second chamber equipped with a TOF mass spectrometer. The laser system consisted of two dye lasers pumped by a doubled Nd:YAG ($\lambda = 532$ nm). The dye fundamental frequencies were doubled and, when necessary, mixed with residual 1064 nm radiation to obtain two different frequencies ν_1 and ν_2. The ions formed by R2PI ionization in the TOF source were mass discriminated and detected by a channeltron after a 50 cm flight path. The photoionization spectra were corrected for the effect of the electric field strength (200 V cm^{-1}) produced by the extraction plates of the TOF spectrometer.[14]

Computational details: The theoretical description of the stable conformers of *R*-(+)-1-phenyl-1-propanol (**R**) was obtained with an IBM RISC/6000 version of the Gaussian 98 set of programs.[16, 17] A full geometry optimization of the investigated conformers was performed at the RHF/3–21G level. Further structural refinement was obtained at the B3LYP/6–31G level of theory with the RHF/3–21G geometries as starting points.[18] Both theoretical approaches provided essentially the same geometries and stability order for the rotamers of **R**, although there was some difference in their relative energy values.

Results and Discussion

Excitation spectrum of the bare chromophore: The mass-resolved 2cR2PI excitation spectrum of the bare chromophore **R** ($m/z = 136$ $[\mathbf{R}]^+$) taken up to 1000 cm^{-1} above its electronic $S_1 \leftarrow S_0$ band origin is shown in Figure 2.[5] The band

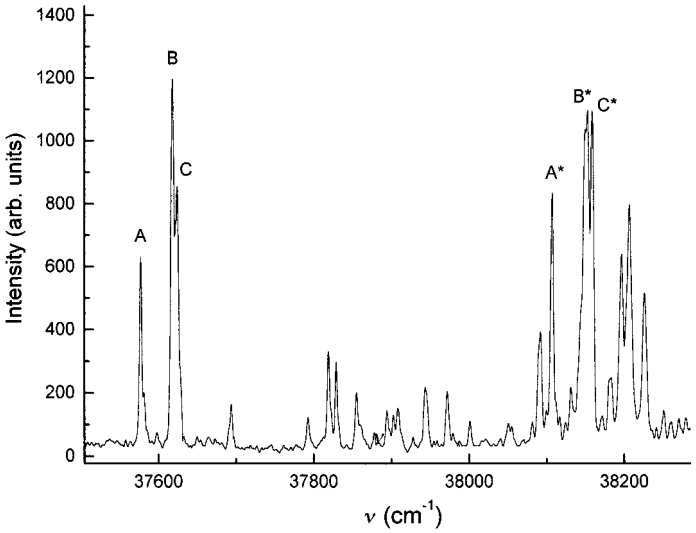

Figure 2. Mass-resolved 2cR2PI excitation spectrum of the bare chromophore *R*-(+)-1-phenyl-1-propanol (**R**), measured at $m/z = 136$ and at a total stagnation pressure of 4×10^5 Pa.

origin region of the spectrum displays a peak at 37577 cm^{-1} (henceforth called A) and two other peaks at 37618 cm^{-1} (henceforth called B) and at 37624 cm^{-1} (henceforth called C). The same triplet is reproduced at 38106 (A*), 38148 (B*), and 38155 cm^{-1} (C*). This pattern is by no means unusual and can be interpreted to be either due to different stable conformers and/or due to their vibronic transitions.[19–21]

To gather some insight into this point, ab initio calculations on the relative stabilities of the conformers of **R** were carried out at the RHF/3–21G and B3LYP/6–31G levels of theory. Three stable structures were identified (Figure 3), with the *anti* rotamer **I** as the global minimum and **III** as the least

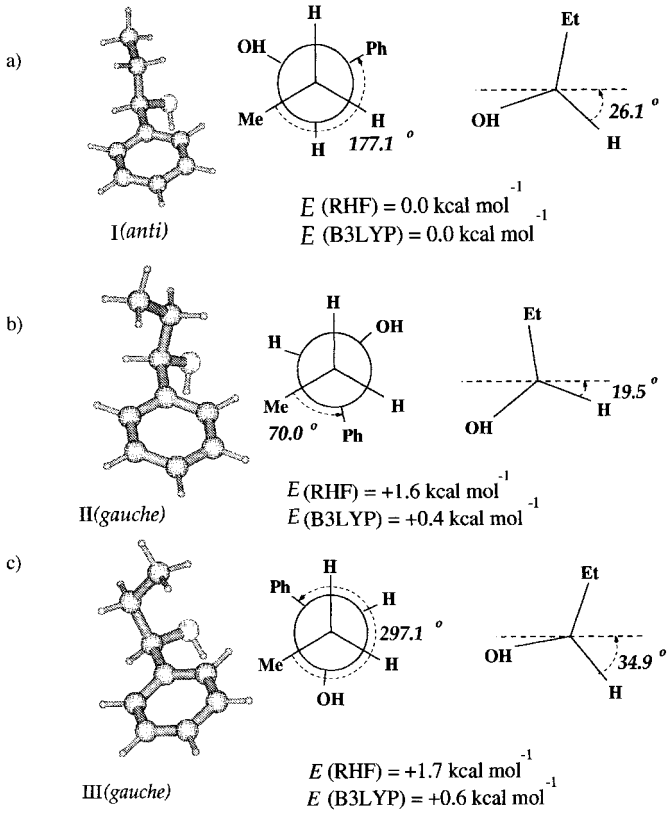

Figure 3. Conformers of the bare chromophore *R*-(+)-1-phenyl-1-propanol (**R**) predicted by RHF/3–21G and B3LYP/6–31G calculations.

stable *gauche* conformer. Both the RHF/3–21G and B3LYP/6–31G energy calculations indicate that all rotamers **I**–**III** are accessible in the expansion; their stability difference ranges from 0.6 (B3LYP/6–31G) to 1.7 kcal mol^{-1} (RHF/3–21G). On these grounds, the most intense band B of Figure 2 may be attributed to the more stable conformer **I**, the second-most intense band A to rotamer **II**, and band C to conformer **III**. Assignment of the three bands to rotamers **I**–**III** is further supported by the match between the intensities of the ABC and the A*B*C* triplets in Figure 2.[21]

Excitation spectra of the molecular complexes: Supersonic expansion of mixtures of alcohols **R** and **solv** generates the corresponding complexes in which the mutual conformations of the **R** and **solv** moieties are determined by the interaction forces. As expected, the presence of all these conformations and the accompanying vibronic transitions heavily complicate the mass-resolved excitation spectra of the isolated complexes, whose interpretation can then be attemped only by resorting to a homologous series of solvent molecules, **solv**. To this purpose, a number of isolated complexes with homologous sets of primary and secondary alcohols **solv** were generated in the supersonic beam, and their mass-resolved excitation spectra were compared. Some of the results are illustrated in Figures 4 and 5.

Figure 4 shows the 1cR2PI excitation spectra of the complexes between **R** and **solv**, with **solv** as the primary alcohols **1**, **2**, **3n**, **4n**, and **5n**, monitored at the m/z values corresponding to their 1:1 adducts [**R**·**solv**]. The major

0947-6539/00/0606-1044 $ 17.50+.50/0 *Chem. Eur. J.* **2000**, *6*, No. 6

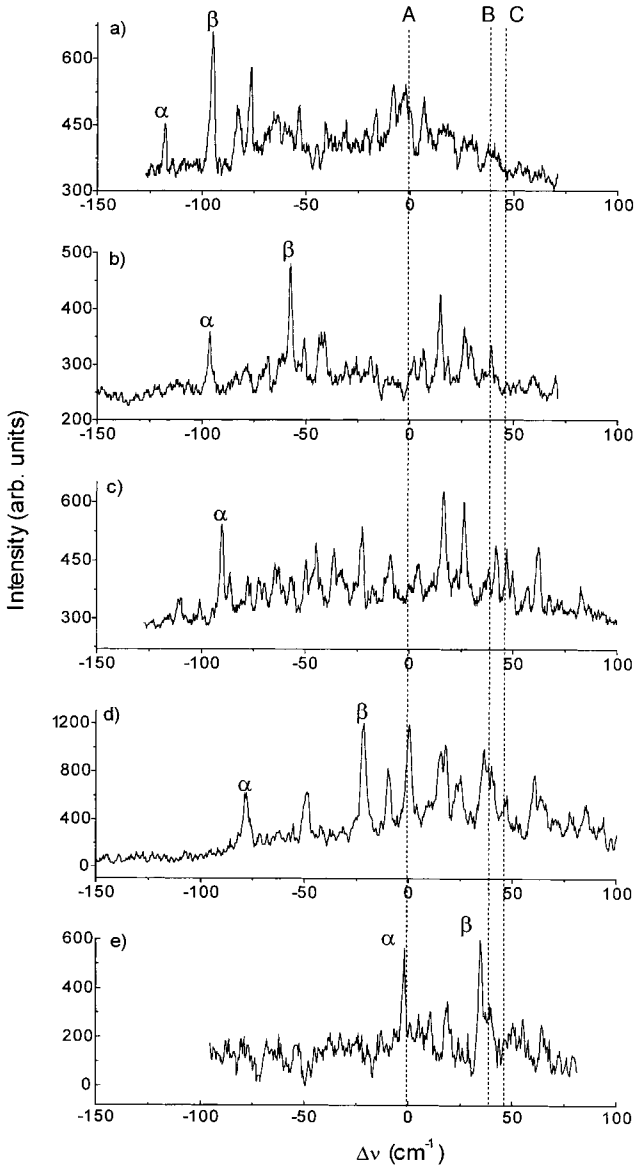

Figure 4. 1cR2PI excitation spectra of the complexes between **R** and a) 1-pentanol, b) 1-butanol, c) 1-propanol, d) ethanol, and e) methanol measured at their m/z value and at a total stagnation pressure of 4×10^5 Pa. The origin of the frequency scale is relative to the electronic band origin A of the $S_1 \leftarrow S_0$ transition of the *gauche* conformer **II** of **R** (Figure 3) at 37577 cm^{-1}.

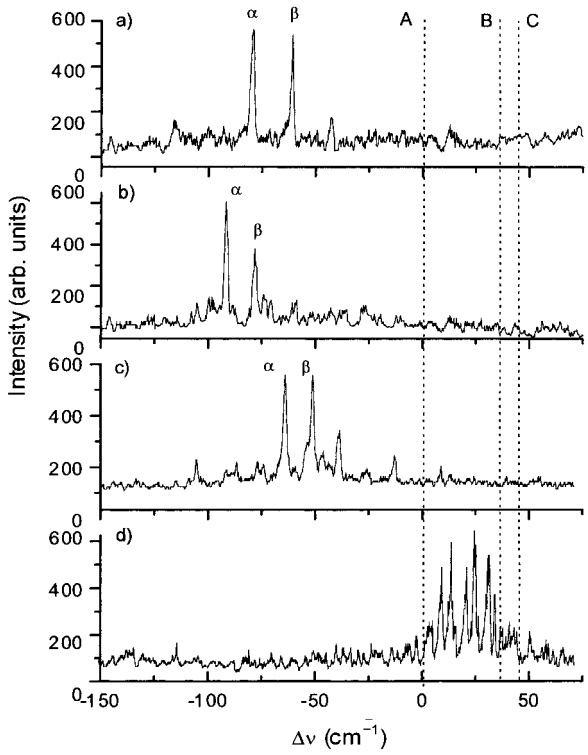

Figure 5. 2cR2PI excitation spectra of the complexes between **R** and a) *R*-(−)-2-butanol, b) *S*-(+)-2-butanol, c) *R*-(−)-2-pentanol, and d) *S*-(+)-2-pentanol measured at their m/z values and at a total stagnation pressure of 4×10^5 Pa. The origin of the frequency scale is relative to the electronic band origin A of the $S_1 \leftarrow S_0$ transition of the *gauche* conformer **II** of **R** (Figure 3) at 37577 cm^{-1}.

characteristic peaks (α and β in Figure 4) in the spectra are shifted relative to the electronic bands A–C of bare **R** (Table 1). The α bands are red-shifted relative to the electronic band A of **R**, by an extent ($\Delta\nu_\alpha$) which increases with increasing length of the R_3 group of **solv**. Red shifts $\Delta\nu_\beta$, similar to the corresponding $\Delta\nu_\alpha$, are observed for the β signals if they are referred to the electronic band B of **R**. Furthermore, the relative intensities of the α and β bands qualitatively parallel that of the A and B electronic bands of **R**. These features lead us to assign the α and β spectral signatures of Figure 4 to two different sets of [**R**·**solv**] conformers, both characterized by the same spatial correlation between the alkyl chain of **solv** and the aromatic ring of **R**. As shown in Figure 6, both $\Delta\nu_\alpha$ and $\Delta\nu_\beta$ are linearly correlated to the proton affinity (PA) of primary **solv** [PA(**solv**) = (180.4 ± 0.6) − (0.076 ± 0.006)$\Delta\nu$, $r^2 = 0.951$] and, hence, to the strength of the O–H···O hydrogen bond between the **R** proton donor and the primary **solv** acceptor.[22] It follows that the different extents of the spectral shifts in Figure 4 reflect the combined effects of electrostatic and dis-

Table 1. R2PI band shifts relative to jet-cooled 1:1 complexes between *R*-(+)-1-phenyl-1-propanol (R2PI) and primary and secondary alcohols (**solv**).

solv	$\Delta\nu_\alpha$ [cm^{-1}][a]	$\Delta\nu_\beta$ [cm^{-1}][a]	PA [kcal mol^{-1}] (see ref. [22])[c]
1cR2PI			
1	−2	−6	180.3
2	−78	−63	185.6
3n	−90	–	188.0
4n	−96	−101	188.6
5n	−118	−136	*189.2*
3i	−87	−71	189.5
5i	−108	–	*195.6*
2cR2PI			
4r	−79	−102	195.0
4s	−92	−119	195.0
5r	−64	−92	*195.6*
5s	ca. +25	–	*195.6*

[a] Band shifts of the α peaks relative to the band origin A of bare **R**; [b] Band shifts of the β peaks relative to the band origin B of bare **R**; [c] Values in italics estimated from the PA limits of primary and secondary alcohols (J. Long, B. Munson, *J. Am. Chem. Soc.* **1977**, *99*, 6822), by using the group additivity method (S. W. Benson, *Thermochemical Kinetics*, Wiley, New York, **1968**).

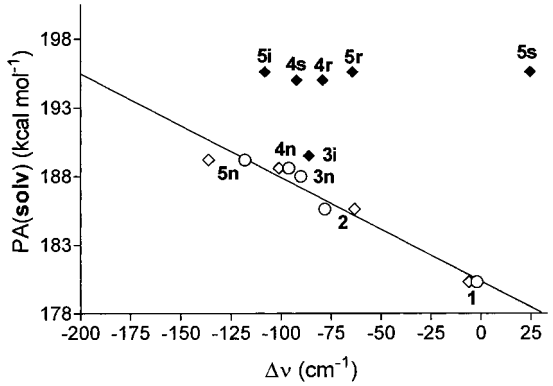

Figure 6. Diagram of band origin shifts $\Delta\nu$ of the selected complexes as a function of the proton affinity (PA) of **solv**. Open circles and diamonds refer to the $\Delta\nu_\alpha$ and $\Delta\nu_\beta$ values of the [**R**·**solv**] adduct, respectively, where **solv** = primary alcohols (see text and Table 1). The full diamonds refer to the $\Delta\nu_\alpha$ values of the [**R**·**solv**] adduct with **solv** = secondary alcohols. The data concerning the relevant $\Delta\nu_\beta$ values are omitted for the sake of clarity.

persive (polarization) interactions on the HOMO and LUMO energies of [**R**·**solv**], in agreement with previous indications.[23]

Figure 5 shows the main features of the 2cR2PI excitation spectra of [**R**·**solv**], in which **solv** is one of the chiral secondary alcohols **4r**, **4s**, **5r**, or **5s**. As for the complexes with primary **solv**, the spectra of the secondary **solv** in Figure 5 exhibit major characteristic α and β peaks that are shifted relative to the electronic bands A – C of bare **R** (Table 1). The relevant $\Delta\nu_\alpha$ and $\Delta\nu_\beta$ shifts are reported in Table 1, together with those from the 1cR2PI excitation spectra of other complexes with secondary alcohols, that is, [**R**·**3i**] and [**R**·**5i**]. All these complexes, except for [**R**·**5s**], have spectral signatures with significant $\Delta\nu_\alpha$ and $\Delta\nu_\beta$ red shifts. The excitation spectrum of [**R**·**5s**] (Figure 5d) is instead characterized by a multiplet that is blue-shifted relative to the band origin A of the bare chromophore **R** ($\Delta\nu$ = ca. $+25$ cm^{-1}). According to Figure 6, the α (as well as the β) signals of the complexes with secondary alcohols have $\Delta\nu$ values that are less negative than expected from the linear correlation obtained for the primary alcohols. These deviations suggest that the relative contributions of the electrostatic and dispersive forces in these systems are substantially different from those that operate in the complexes with primary **solv**. The extent of these deviations actually depends on the bulkiness and the spatial orientation of the alkyl chains of secondary **solv**. This provides the first inkling that, in the adducts with secondary **solv**, steric factors somewhat reduce the effect of the attractive electrostatic and dispersive interactions on the HOMO – LUMO gap of the adduct.

Particularly intriguing, from this perspective, are the different deviations observed for the diastereomeric [**R**·**4r**]/[**R**·**4s**] and [**R**·**5r**]/[**R**·**5s**] pairs. The $\Delta\nu_\alpha([\mathbf{R}\cdot\mathbf{4r}]) = -79$ cm^{-1} and $\Delta\nu_\alpha([\mathbf{R}\cdot\mathbf{4s}]) = -92$ cm^{-1} red shifts of the α bands in Table 1 indicate that the binding energy of both adducts is greater in the S_1 state than in the S_0 state.[7] The same rationale applies to the $\Delta\nu_\alpha([\mathbf{R}\cdot\mathbf{5r}]) = -64$ cm^{-1} red shift , whereas the multiplet of signals of [**R**·**5s**], blue-shifted by ca. $+25$ cm^{-1} from the $S_1 \leftarrow S_0$ band origin A of bare **R**, is accounted for by an $S_1 \leftarrow S_0$ transition in [**R**·**5s**] involving a decrease of its binding energy. The difference $\Delta\Delta\nu_\alpha = h\nu_1[\mathbf{R}\cdot\mathbf{4r}]^* - h\nu_1[\mathbf{R}\cdot\mathbf{4s}]^* = +13$ cm^{-1} reflects that the $S_1 \leftarrow S_0$ energy gap of the heterochiral complex is smaller than that of the corresponding homochiral one. The trend is just the opposite for the [**R**·**5r**]/[**R**·**5s**] pairs, for which $\Delta\Delta\nu = h\nu_1[\mathbf{R}\cdot\mathbf{5r}]^* - h\nu_1[\mathbf{R}\cdot\mathbf{5s}]^* =$ ca. -89 cm^{-1}. The opposite sign and magnitude of the $\Delta\Delta\nu$ values measured for the diastereomeric [**R**·**4r**]/[**R**·**4s**] and [**R**·**5r**]/[**R**·**5s**] pairs support the view that the HOMO – LUMO gap in [**R**·**solv**] complexes with secondary alcohols is considerably affected by steric factors.

The $\Delta\Delta\nu_\alpha = h\nu_1[\mathbf{R}\cdot\mathbf{4r}]^* - h\nu_1[\mathbf{R}\cdot\mathbf{4s}]^* = +13$ cm^{-1} difference corresponds closely with the greater LIF red shift of the heterochiral complex between *R*-(+)-2-naphthyl-1-ethanol (**N**) and **4s**, compared with that measured for the homochiral [**N**·**4r**] complex.[1–3] However, although the LIF results for the [**N**·**5r**]/[**N**·**5s**] pair[1–3] are qualitatively similar to those of [**N**·**4r**]/[**N**·**4s**], there is no correspondence with the $\Delta\Delta\nu = h\nu_1[\mathbf{R}\cdot\mathbf{5r}]^* - h\nu_1[\mathbf{R}\cdot\mathbf{5s}]^* =$ ca. -89 cm^{-1}. This marked spectral diversity can be attributed to the shorter side chain and the wider "π-electron bed" of **N**, relative to **R**; this allows a good compromise between attractive dispersive and repulsive steric interactions with **solv** in both the S_0 and S_1 states. In the corresponding complexes with **R**, the same good compromise is prevented by the comparatively bulkier side chain and narrower π system of the chromophore, and the repulsive forces can, therefore, play a much more "visible" role in both the ground and excited states.

The different 2cR2PI spectroscopic features of the diastereomeric [**R**·**4r**]/[**R**·**4s**] and [**R**·**5r**]/[**R**·**5s**] pairs are mirrored by their 1cR2PI/TOF mass spectral patterns, taken at $\nu_1 = 37485$ ([**R**·**4s**]), 37498 ([**R**·**4r**]), 37597 ([**R**·**5s**]), and 37513 cm^{-1} ([**R**·**5r**]). The heterochiral diastereomers of both pairs are invariably characterized by more extensive fragmentation.

Binding energy of the molecular complexes: Some insights into the forces operating in the selected MC can be obtained from their binding energies, measured by using the procedure summarized in Figure 7.

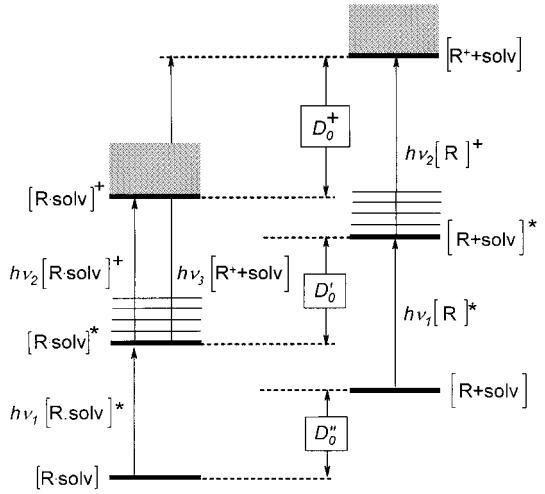

Figure 7. Schematic representation of the energy levels of the [**R**·**solv**] adduct (left-hand side) and of the bare chromophore **R** (right-hand side). The symbols in the squares refer to the binding energy of [**R**·**solv**] (D_o''), [**R**·**solv**]* (D_o'), and [**R**·**solv**]$^+$ (D_o^+) adducts. Excitation ($h\nu_1$), ionization ($h\nu_2$), and dissociative ionization ($h\nu_3$) energies are as reported in Table 2, with the same notations.

0947-6539/00/0606-1046 $ 17.50+.50/0 *Chem. Eur. J.* **2000**, *6*, No. 6

The binding energy D_0'' of the [**R·solv**] adducts, as determined by 2cR2PI experiments, is computed from Equation (1), namely from the difference between its dissociative ionization threshold ($AE(\mathbf{R}^+) = h\nu_1([\mathbf{R}\cdot\mathbf{solv}]^*) + h\nu_3([\mathbf{R}^+ + \mathbf{solv}])$; Figure 7) and the ionization threshold of bare **R** ($IP(\mathbf{R}) = h\nu_1([\mathbf{R}]^*) + h\nu_2([\mathbf{R}]^+)$ [IP = appearance potential; AE = dissociative appearance potential].

$$D_0'' = h\nu_1([\mathbf{R}\cdot\mathbf{solv}]^*) + h\nu_3([\mathbf{R}^+ + \mathbf{solv}]) - IP(\mathbf{R}) \quad (1)$$

The binding energy D_0' of the excited [**R·solv**]* adducts is taken as equal to $D_0'' - \Delta\nu$; the appropriate $\Delta\nu$ terms from Table 1 are used. The dissociation energy D_0^+ of the ionic cluster $[\mathbf{R}\cdot\mathbf{solv}]^+$ is calculated from Equation (2), namely from the difference between its dissociative ionization threshold ($AE(\mathbf{R}^+) = h\nu_1([\mathbf{R}\cdot\mathbf{solv}]^*) + h\nu_3([\mathbf{R}^+ + \mathbf{solv}])$; Figure 7) and its ionization threshold ($IP([\mathbf{R}\cdot\mathbf{solv}]) = h\nu_1([\mathbf{R}\cdot\mathbf{solv}]^*) + h\nu_2([\mathbf{R}\cdot\mathbf{solv}]^+)$).

$$D_0^+ = (h\nu_1([\mathbf{R}\cdot\mathbf{solv}]^*) + h\nu_3([\mathbf{R}^+ + \mathbf{solv}]) - IP([\mathbf{R}\cdot\mathbf{solv}] = h\nu_3([\mathbf{R}^+ + \mathbf{solv}]) - h\nu_2([\mathbf{R}\cdot\mathbf{solv}]^+) \quad (2)$$

The 2cR2PI ionization threshold of bare **R** is shown in Figure 8a. The rise of the $\mathbf{R}^+$ signal intensity with ν_2 appears rather broad. This is attributable to a change of molecular geometry upon ionization. The threshold of the $\mathbf{R}^+$ signal is taken by setting ν_1 at the frequencies corresponding to bands A–C (band: 37577.3 cm^{-1}(A); 37618 (B); 37624 (C)). All these measurements provide the same value for the appearance potential of $\mathbf{R}^+$ (8.84 eV) within the experimental uncertainty (±0.01 eV).

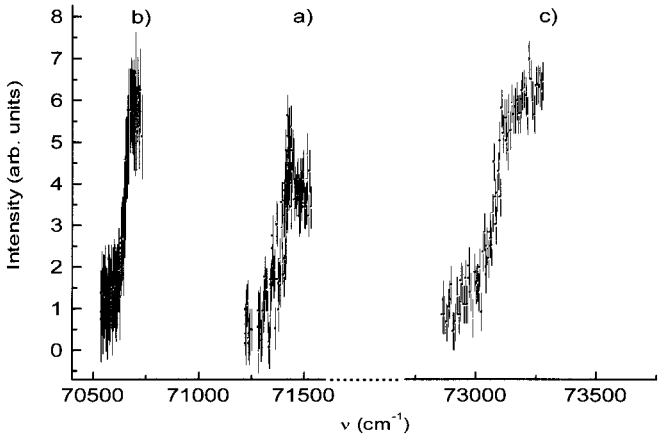

Figure 8. a) 2cR2PI ionization threshold of bare **R**, measured at $m/z = 136$; b) 2cR2PI ionization threshold of [**R·4s**], measured at $m/z = 210$; c) 2cR2PI dissociative ionization threshold of [**R·4s**], measured at $m/z = 210$ (total stagnation pressure of 4×10^5 Pa). Intensity, I, is given in arbitrary units; $\nu = \nu_1 + \nu_2$ for a) and b); $\nu = \nu_1 + \nu_3$ for c) (see Table 2).

The 2cR2PI ionization and dissociative ionization thresholds of [**R·4s**] are illustrated in Figure 8b and 8c, respectively. Similar ionization and dissociative ionization thresholds are obtained for [**R·3i**], [**R·4n**],[7] [**R·4r**],[7] [**R·5r**], and [**R·5s**]. The relevant appearance potential (IP) and dissociative appearance potential (AE) are listed in Table 2, together with their derived D_0'', D_0', and D_0^+ dissociation energies. The D_0'' value of [**R·4n**] (2.6 ± 0.2 kcal mol^{-1}) agrees well with an approximate estimate of the dissociation energy of the complex between *R*-(+)-2-naphthyl-1-ethanol (**N**) and another primary alcohol, namely methanol (**1**) ($D_0''([\mathbf{N}\cdot\mathbf{1}]) = 2$–3 kcal mol^{-1}), obtained by comparing the dispersed fluorescence emission spectra of **N** arising from excitation of bare **N** with that of the [**N·1**] adduct.[2] The higher D_0'' values measured for the complexes between **R** and the selected secondary alcohols agree completely with the expected increase of the O–H···O hydrogen bond strength with the proton affinity (PA) of **solv** (Table 1). The $\Delta = D_0''([\mathbf{R}\cdot\mathbf{4r}]) - D_0''([\mathbf{R}\cdot\mathbf{4s}]) = 1.1 \pm 0.4$ kcal mol^{-1} and $\Delta = D_0''([\mathbf{R}\cdot\mathbf{5r}]) - D_0''([\mathbf{R}\cdot\mathbf{5s}]) = 1.6 \pm 0.4$ kcal mol^{-1} values in Table 2 demonstrate that the homochiral complexes are appreciably more stable toward dissociation than the heterochiral ones. This trend extends to the corresponding S_1-excited complexes as well, that is, $\Delta^* = D_0'([\mathbf{R}\cdot\mathbf{4r}]) - D_0'([\mathbf{R}\cdot\mathbf{4s}]) = \Delta - 13$ cm^{-1} $= 350$ cm^{-1} (1.0 ± 0.4 kcal mol^{-1}) and $\Delta^* = D_0'([\mathbf{R}\cdot\mathbf{5r}]) - D_0'([\mathbf{R}\cdot\mathbf{5s}]) = \Delta + 89$ $cm^{-1} = 630$ cm^{-1} (1.8 ± 0.4 kcal mol^{-1}).

As pointed out before, the binding energies of the ground- and the excited-state [**R·4r**], [**R·4s**], [**R·5r**], [**R·5s**], and [**R·3i**] adducts are higher than those of [**R·4n**] and [**N·1**] and reflect the comparatively more intense attractive electrostatic forces operating in the complexes with secondary **solv** moieties.[1, 2, 4] However, the $\Delta\nu$ deviation from linearity in Figure 6, coupled with the different shifts of the electronic band origin of the diastereomeric [**R·4r**]/[**R·4s**] and [**R·5r**]/[**R·5s**] pairs involving equally basic **solv** ($\Delta - \Delta^* = +13$ and -89 cm^{-1}, respectively), corroborates the view that the interaction forces in these diastereomeric MCs respond to repulsive steric factors to different extents. This differing sensitivity is demonstrated by the following diverging obser-

Table 2. Wavenumbers for excitation (ν_1), threshold ionization (ν_2), and threshold dissociative ionization (ν_3) of bare chromophore **R** and its complexes with **solv** molecules. Ionization potentials (IP), appeareance potentials (AE), and dissociation energies of fundamental (D_0''), excited (D_0') and ionic state (D_0^+) of complexes. All values are in cm^{-1}, figures in parentheses are in kcal mol^{-1} (1 kcal mol^{-1} = 349.77 cm^{-1}).

	ν_1 ($S_1 \leftarrow S_0$)	$\Delta\nu$	ν_2	IP[a] $\nu_1 + \nu_2$	ΔIP	ν_3	AE[a] $\nu_1 + \nu_3$	D_0'' AE – IP(**R**)	D_0' ($D_0'' - \Delta\nu$)	$D(D_0^+ - \Delta\nu)$ ($D_0'' - \Delta$IP)
[**R**]	37577 ± 1	–	33670 ± 40	71330 ± 40	–	–	–	–	–	–
[**R·3i**]	37490 ± 1	−87 ± 2	–	–	–	35030 ± 40	72610 ± 40	1280 ± 80 (3.7 ± 0.2)	1370 ± 80 (3.9 ± 0.2)	–
[**R·4n**]	37520 ± 1	−96 ± 2	32380 ± 40	69980 ± 40	−1350 ± 80	34640 ± 40	72240 ± 40	910 ± 80 (2.6 ± 0.2)	1010 ± 80 (2.9 ± 0.2)	2260 ± 80 (6.5 ± 0.2)
[**R·4s**]	37485 ± 1	−92 ± 2	33070 ± 40	70640 ± 40	−690 ± 80	35455 ± 40	73020 ± 40	1690 ± 80 (4.8 ± 0.2)	1780 ± 80 (5.1 ± 0.2)	2380 ± 80 (6.8 ± 0.2)
[**R·4r**]	37498 ± 1	−79 ± 2	32860 ± 40	70440 ± 40	−890 ± 80	35800 ± 40	73380 ± 40	2050 ± 80 (5.9 ± 0.2)	2130 ± 80 (6.1 ± 0.2)	2940 ± 80 (8.4 ± 0.2)
[**R·5s**]	37602 ± 1	+25 ± 2	33140 ± 40	70820 ± 40	−510 ± 80	34750 ± 40	72430 ± 40	1100 ± 80 (3.1 ± 0.2)	1070 ± 80 (3.1 ± 0.2)	1610 ± 80 (4.6 ± 0.2)
[**R·5r**]	37513 ± 1	−64 ± 2	32390 ± 40	69990 ± 40	−1340 ± 80	35370 ± 40	72970 ± 40	1640 ± 80 (4.7 ± 0.2)	1700 ± 80 (4.9 ± 0.2)	2980 ± 80 (8.5 ± 0.2)

[a] After correction for TOF field ionization energy (+85 cm^{-1}).

vations (Table 2): i) For the diastereomeric [**R·4r**]/[**R·4s**] pair, the larger red shift is associated with the less stable heterochiral complex [**R·4s**]; ii) For the diastereomeric [**R·5r**]/[**R·5s**] pair, the less stable heterochiral complex [**R·5s**] exhibits a blue shift and the most stable homochiral complex [**R·5r**] undergoes a red shift.

The lower D_0'' values of the heterochiral complexes relative to the values of the corresponding homochiral adducts (Table 2) point to a more pronounced steric congestion in the former diastereomers. However, the $\Delta - \Delta^* = +13\ cm^{-1}$ difference in shifts, measured for the [**R·4r**]/[**R·4s**] pair, indicates that the $S_1 \leftarrow S_0$ transition is accompanied by a higher increase of dispersive interactions in the heterochiral [**R·4s**] adduct than in the more stable homochiral homologue, despite the higher steric congestion in the first complex. The pattern is completely reversed for the [**R·5r**]/[**R·5s**] pair. Here, comparison of the red shifts of the α and β signals of the homochiral [**R·5r**] adduct with the more pronounced red shifts of the [**R·4r**] complex suggests that the increase of dispersive interactions accompanying the $S_1 \leftarrow S_0$ transition in the sterically more congested [**R·5r**] ($D_0''([\mathbf{R\cdot 5r}]) = 4.7 \pm 0.2\ kcal\,mol^{-1}$) is less pronounced than that for the less congested [**R·4r**] homologue ($D_0''([\mathbf{R\cdot 4r}]) = 5.9 \pm 0.2\ kcal\,mol^{-1}$). This situation goes to extremes in the less stable heterochiral [**R·5s**] adduct. The blue shift accompanying the $S_1 \leftarrow S_0$ transition in this complex is accounted for by its high steric congestion (cf. $D_0''([\mathbf{R\cdot 5r}]) = 4.7 \pm 0.2\ kcal\,mol^{-1}$ vs. $D_0''([\mathbf{R\cdot 5s}]) = 3.1 \pm 0.2\ kcal\,mol^{-1}$); this allows spatial arrangement of the two moieties to favor mostly the attractive electrostatic forces (e.g., O–H$\cdots\pi$-ring) rather than dispersive interactions.[24]

Inspection of the data in Table 2 reveals that the D_0^+ values, measured for the ionic complexes $[\mathbf{R\cdot solv}]^+$, always exceed the D_0'' interaction energies of their neutral counterparts. Determination of D_0^+ is of some interest in view of the paucity of literature binding energies of isolated complexes, in particular hydrogen-bonded complexes, formed between arene radical cations and polar molecules. In this context, the absolute D_0^+ values of Table 2 seem too low relative to the binding energy between the π-system of an arene radical cation and a butanol molecule, estimated to exceed $12\ kcal\,mol^{-1}$.[25] Several factors can account for this discrepancy. One is that there is a significant change in the equilibrium configuration of the complex in its excited and ionic state, to result in a vertical $h\nu_2([\mathbf{R\cdot solv}]^+)$ absorption exceeding the corresponding 0^0_0 transition. Another refers to the possibility that the vertical $h\nu_2([\mathbf{R\cdot solv}]^+)$ transition mostly populates the hydrogen-bonded local minimum of the $[\mathbf{R\cdot solv}]^+$ potential energy surface, which is separated from the global π-bonded one by a significant energy barrier. Work is in progress to settle this point.

The vertical D_0^+ values in Table 2 qualitatively parallel the corresponding D_0'' energies. For instance, the D_0^+ values of the homochiral complexes $[\mathbf{R\cdot 4r}]^+$ and $[\mathbf{R\cdot 5r}]^+$ are significantly higher than those of the corresponding heterochiral adducts. However, comparison of $\Delta = D_0''([\mathbf{R\cdot 4r}]) - D_0''([\mathbf{R\cdot 4s}]) = 1.1 \pm 0.4\ kcal\,mol^{-1}$ and $\Delta^+ = D_0^+([\mathbf{R\cdot 4r}]) - D_0^+([\mathbf{R\cdot 4s}] = 1.6 \pm 0.4\ kcal\,mol^{-1}$, on the one hand, and $\Delta = D_0''([\mathbf{R\cdot 5r}]) - D_0''([\mathbf{R\cdot 5s}]) = 1.4 \pm 0.4\ kcal\,mol^{-1}$ and $\Delta^+ = D_0^+([\mathbf{R\cdot 5r}]) - D_0^+([\mathbf{R\cdot 5s}] = 3.9 \pm 0.4\ kcal\,mol^{-1}$, on the other, reveals that the extra stabilization due to ionization is always larger for the more stable homochiral complexes [**R·4r**] and [**R·5r**] (Table 2). These findings conform to the view that the comparatively high steric congestion in the heterochiral [**R·4s**] and [**R·5s**] complexes hinders development of strong electrostatic interactions after ionization. This occurs to an extent that is significantly larger than in the corresponding homochiral [**R·4r**] and [**R·5r**] adducts, and this hindrance is more pronounced in the highly congested [**R·5s**] adduct than in the less congested [**R·4s**] analogue.

In conclusion, the R2PI/TOF technique has been applied for the first time to explore the nature of the forces acting in MCs between a chiral aromatic alcohol (**R**) and a set of primary and secondary aliphatic alcohols (**solv**) generated in a supersonic molecular beam. There is a subtle interplay between the attractive (electrostatic and polarization) and repulsive (steric) interactions in the ground and excited [**R·solv**] complexes; this interplay depends on the structure and the configuration of **solv**. The 2cR2PI/TOF technique has proved to be an excellent tool for enantiodifferentiating chiral **solv** molecules through the spectral and energetic features of their *neutral* and *ionic* [**R·solv**] adducts with a suitable aromatic chromophore **R**. Of the systems investigated, the homochiral complexes were found to be invariably more stable than the heterochiral ones, both in the ground and the excited states. The same is true for the corresponding ionic adducts. The stability differences of the neutral adducts was traced to differences in the alkyl-group configurations and to different steric requirements during complexation.

Acknowledgments

This work was supported by the Ministero della Università e della Ricerca Scientifica e Tecnologica (MURST) and the Consiglio Nazionale delle Ricerche (CNR). M.S. acknowledges Michael Mautner for helpful discussions on the binding energies between arene radical ions and polar molecules. The help and the advice of Fulvio Cacace are gratefully acknowledged.

[1] A. R. Al-Rabaa, E. Bréhéret, F. Lahmani, A. Zehnacker-Rentien, *Chem. Phys. Lett.* **1995**, *237*, 480.
[2] A. R. Al-Rabaa, K. Le Barbu, F. Lahmani, A. Zehnacker-Rentien, *J. Phys. Chem.* **1997**, *101*, 3273.
[3] K. Le Barbu, V. Brenner, P. Millié, F. Lahmani, A. Zehnacker-Rentien, *J. Phys. Chem. A* **1998**, *102*, 128.
[4] S. Piccirillo, C. Bosman, D. Toja, A. Giardini-Guidoni, M. Pierini, A. Troiani, M. Speranza, *Angew. Chem.* **1997**, *109*, 1816; *Angew. Chem. Int. Ed. Engl.* **1997**, *36*, 1729.
[5] A. Giardini Guidoni, S. Piccirillo, *Isr. J. Chem.* **1997**, *37*, 439.
[6] A. Latini, D. Toja, A. Giardini-Guidoni, A. Palleschi, S. Piccirillo, M. Speranza, *Chirality* **1999**, *11*, 376.
[7] A. Latini, D. Toja, A. Giardini-Guidoni, S. Piccirillo, M. Speranza, *Angew. Chem.* **1999**, *111*, 838; *Angew. Chem. Int. Ed.* **1999**, *38*, 815; See also, H. J. Neusser, H. Krause, *Chem. Rev.* **1994**, *94*, 1829, and references therein.
[8] N. Ramsey, *Molecular Beams*, Oxford Clarendon Press, Oxford, **1956**.
[9] R. E. Smalley, B. L. Ramakrishna, D. H. Levy, L. Wharton, *J. Chem. Phys.* **1974**, *61*, 4363.
[10] W. C. Wiley, I. H. McLaren, *Rev. Sci. Instrum.* **1955**, *26*, 1150.
[11] B. Brutschy, *Chem. Rev.* **1992**, *92*, 1567.

  0947-6539/00/0606-1048 $ 17.50+.50/0 *Chem. Eur. J.* **2000**, *6*, No. 6

[12] M. Coreno, S. Piccirillo, A. Giardini Guidoni, A. Mele, A. Palleschi, P. Brechignac, P. Parneix, *Chem. Phys. Lett.* **1995**, *236*, 580.
[13] S. Piccirillo, M. Coreno, A. Giardini-Guidoni, G. Pizzella, M. Snels, R. Teghil, *J. Mol. Struct.* **1993**, *293*, 197.
[14] T. M. Di Palma, A. Latini, M. Satta, M. Varvesi, A. Giardini Guidoni, *Chem. Phys. Lett.* **1998**, *284*, 184.
[15] D. Consalvo, A. van der Avoird, S. Piccirillo, M. Coreno, A. Giardini-Guidoni, A. Mele, M. Snels, *J. Chem. Phys.* **1993**, *99*, 8398.
[16] M. J. Frish, G. W. Trucks, H. B. Schlegel, P. M. W. Gill, B. G. Johnson, M. A. Robb, J. R. Cheeseman, T. A. Keith, G. A. Petersson, J. A. Montgomery, K. Ragavachari, M. A. Al-Laham, V. G. Zakrzewski, J. V. Ortiz, J. B. Foresman, J. Cioslowski, B. B. Stefanov, A. Nanayakkara, M. Challacombe, C. Y. Peng, P. Y. Ayala, W. Chen, M. W. Wong, J. L. Andres, E. S. Repogle, R. Gomperts, R. L. Martin, D. J. Fox, J. S. Binkley, D. J. Defrees, J. Baker, J. J. P. Stewart, M. Head-Gordon, C. Gonzales, J. A. Pople, *GAUSSIAN 94, Revision C.2*, Gaussian, Pittsburgh, PA, **1995**.
[17] C. Peng, H. B. Schlegel, *Isr. J. Chem.* **1993**, *33*, 449.
[18] A. D. Becke, *J. Chem. Phys.* **1993**, *98*, 1372, 5648.
[19] S. Sun, E. R. Bernstein, *J. Am. Chem. Soc.* **1996**, *118*, 5086.
[20] S. Li, E. R. Bernstein, *J. Chem. Phys.* **1992**, *97*, 7383.
[21] Vibronic bands around 530 cm^{-1} above the electronic $S_1 \leftarrow S_0$ origin ($6b_0^1$) characterize the spectrum of many substituted benzenes and are found to be independent of the nature of the substituent; cf. J. B. Hopkins, D. E. Powers, S. Mukamel, R. E. Smalley, *J. Chem. Phys.* **1980**, *72*, 5049.
[22] In general, the hydrogen-bond strength increases with the acidity of the donor (ΔH^0_{acid}) and the proton affinity (PA) of the acceptor (F. Hibbert, J. Emsley, *Adv. Phys. Org. Chem.* **1990**, *26*, 225). No thermochemical data are presently available on the relative gas-phase acidity of 2-naphthyl-1-ethanol and 1-phenyl-1-propanol. However, the former alcohol should be appreciably less acidic than the latter, if one considers that the ΔH^0_{acid} of ethanol is 1.8 kcal mol^{-1} more than that of 1-propanol (M. J. Haas, A. G. Harrison, *Int. J. Mass Spectrom. Ion Proc.* **1993**, *124*, 115) and that the differential effects of the aromatic substituents on their acidity approximately cancels out (J. E. Bartmess, J. A. Scott, R. T. McIver, Jr., *J. Am. Chem. Soc.* **1979**, *101*, 6046, 6056). The proton affinities (PA) of **solv** are reported in S. G. Lias, J. E. Bartmess, J. F. Liebman, J. L. Holmes, R. D. Levin, W. G. Mallard, *J. Phys. Chem. Ref. Data* **1988**, *17*, Suppl. 1.
[23] E. R. Bernstein, in *Atomic and Molecular Clusters* (Ed.: E. R. Bernstein), Elsevier, Amsterdam, **1990**.
[24] An alternative effect of the steric congestion in [**R**·**5s**] may be a change in the nature of the O–H ··· O hydrogen bond, wherein **5s** acts as the donor and **R** as the acceptor.
[25] Estimated on the grounds of the experimental value of 7.3 kcal mol^{-1} for the complex of $C_6H_6^+$ with the polar, but less polarizable HCl molecule (E. A. Walters, J. R. Grover, M. White, E. Hui, *J. Phys. Chem.* **1985**, *89*, 3841) and of 12.2 kcal mol^{-1} for that with the nonpolar, but polarizable CS_2 molecule (M. Meot-Ner (Mautner), P. Hamlet, E. P. Hunter, F. H. Field, *J. Am. Chem. Soc.* **1978**, *100*, 5466).

Received: July 13, 1999 [F1911]